



**HAL**  
open science

# Single Event Effects Analysis in Readout Integrated Circuits at Cryogenic Temperatures

Laurent Artola, S. Ducret, Ahmad Al Youssef, R. Buiron, F. Perrier,  
Guillaume Hubert, C. Poivey

► **To cite this version:**

Laurent Artola, S. Ducret, Ahmad Al Youssef, R. Buiron, F. Perrier, et al.. Single Event Effects Analysis in Readout Integrated Circuits at Cryogenic Temperatures. AMICSA 2018, Jun 2018, LOUVAIN, Belgium. hal-01957135

**HAL Id: hal-01957135**

**<https://hal.science/hal-01957135>**

Submitted on 17 Dec 2018

**HAL** is a multi-disciplinary open access archive for the deposit and dissemination of scientific research documents, whether they are published or not. The documents may come from teaching and research institutions in France or abroad, or from public or private research centers.

L'archive ouverte pluridisciplinaire **HAL**, est destinée au dépôt et à la diffusion de documents scientifiques de niveau recherche, publiés ou non, émanant des établissements d'enseignement et de recherche français ou étrangers, des laboratoires publics ou privés.

# Single Event Effects Analysis in Readout Integrated Circuits at Cryogenic Temperatures

L. Artola<sup>1</sup>, S. Ducret<sup>2</sup>, A. Al Youssef<sup>1,2</sup>, R. Buiron<sup>2</sup>, F. Perrier<sup>2</sup>, G. Hubert<sup>1</sup>, C. Poivey<sup>3</sup>

<sup>1</sup> ONERA, Toulouse, France

<sup>2</sup> Sofradir, Veurey-Voroize, France

<sup>3</sup> European Space Agency ESTEC, Netherlands

[laurent.artola@onera.fr](mailto:laurent.artola@onera.fr)

## Abstract

This work presents the analyses of single event transients and functional interrupts measured on two designs of readout integrated circuit under a heavy ions beam cooled down at cryogenic temperatures. The analysis of the multiplicity of SETs in the pixel arrays is completed by means of the SEE prediction tool, MUSCA SEP3.

## I. INTRODUCTION

Complementary metal oxide semiconductor (CMOS) technology is widely used in image sensors and infrared detector onboard launchers or satellites [1]. Actually, many optical applications, like Earth or space observation, the guidance system in a spacecraft are particularly critical. Photonic imager technology has been developed for various wavelengths from ultraviolet, through visible, to infrared. For IR detectors, the MCT material (AgCdTe) is used for the detection circuit. The detection circuit is hybridized on a CMOS circuit which performs the transfer and the control of the IR detector. The CMOS technology used in the readout circuit (ROIC) improves the integration of electronics function and reduce the dark current. A readout circuit is composed by vertical decoders, multiplexers, sequencer, and various logics and sequential cells.

However, these digital CMOS functions of image sensors are known to be sensitive to single event effects (SEE), such as single event transient (SET) or Single Event Functional Interrupt (SEFI) [2]. SETs can be induced by various ionizing particles, i.e., especially heavy ions and protons for the space environment space.

The first goal of this paper is to present the impact or not of cryogenic temperatures on SET and SEFI induced by heavy ions on two different readout circuits of IR image sensors developed by Sofradir.

The second goal is to analyze the multiplicity of SETs and to determine the origin of such events by the mean of the prediction tool MUSCA SEP3 (MUti-SCALE Single Event Phenomena Prediction Platform) [3][4]. Such analyze is relevant with the aim to anticipate the SEE sensitivity trends and propose new radiation tests protocol for IR detectors.

## II. RADIATION TEST OF ROIC UNDER HEAVY IONS AT CRYOGENIC TEMPERATURES

### A. Irradiation test setup

The irradiation test campaigns were performed at UCL (Université Catholique de Louvain - Belgium) with the heavy ion test facility. The CYCotron of Louvain la NEuve (CYCLONE) proposes different heavy ions species which are split in two "Ion cocktails", named M/Q= 5 and M/Q 3.3. The heavy ion species are summarized in Table 1 and Table 2. It has been confirmed (by SRIM simulations) that the penetration depth of the ions is enough to reach the sensitivity areas through the device layers.

**Table 1:** UCL ions cocktail M/Q=5

Ion	Energie (MeV)	Range ( $\mu\text{m}(\text{Si})$ )	LET ( $\text{MeV}\cdot\text{cm}^2/\text{mg}$ )
<sup>15</sup> N <sup>3+</sup>	60	59	3.3
<sup>20</sup> Ne <sup>4+</sup>	78	45	6.4
<sup>40</sup> Ar <sup>8+</sup>	151	40	15.9
<sup>84</sup> Kr <sup>17+</sup>	305	39	40.4
<sup>124</sup> Xe <sup>25+</sup>	420	37	67.7

**Table 2 :** UCL ions cocktail M/Q=3.3

Ion	Energie (MeV)	Range ( $\mu\text{m}(\text{Si})$ )	LET ( $\text{MeV}\cdot\text{cm}^2/\text{mg}$ )
<sup>13</sup> C <sup>4+</sup>	131	292	1.1
<sup>22</sup> Ne <sup>7+</sup>	235	216	3
<sup>40</sup> Ar <sup>12+</sup>	372	117	10.2
<sup>58</sup> Ni <sup>18+</sup>	567	100	20.4
<sup>83</sup> Kr <sup>25+</sup>	756	92	32.6

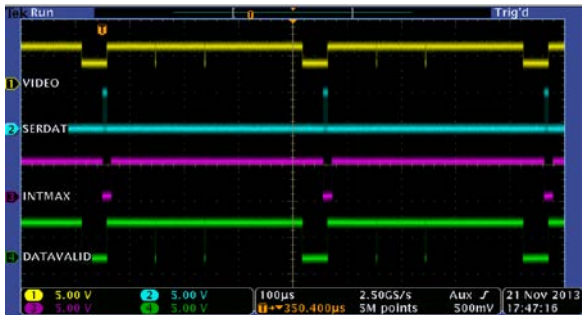
During all the testing measurements, the temperature of the chip was monitored and regulated by a cryostat to a range of temperature from 50K to 300K. During the complete irradiation campaign a GUARD (Graphical Universal

Autorange Delatcher) device has been used on the DUT's power in order to detect Single Event Latchup (SEL) and to prevent its destruction [5]. The global views of the experimental setups used during this irradiation campaign are shown in Figure 1:. The chamber has the shape of a barrel stretched vertically; its internal dimensions are 71 cm in height, 54 cm in width and 76 cm in depth. One side flange is used to support the board frame (25 x 25 cm<sup>2</sup>) and user connectors. The chamber is equipped with a vacuum system. In the case of the campaign the DUT is in a cryostat connected to the vacuum chamber in order to allow for cooling the temperature of the chip during the irradiation test.

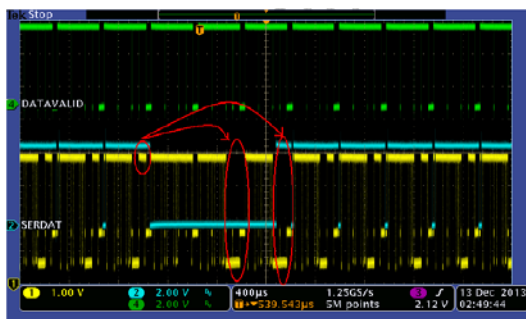
### Cryostat



Figure 1: Global view of the SEE experimental setup of ROIC tested at UCL heavy ion facility in Louvain La Neuve, Belgium



(a)



(b)

Figure 2: (a) Reference levels of monitored signals, (b) Detection of SEFI observed on DATAVALID signal (green line), VIDEO signal (yellow line) and its consequence on the SERDAT signal (serial link, (blue line)) of the ROIC during heavy ion irradiation

### B. Description of the device under test

The DUT during this irradiation test campaign was a readout integrated circuit. Three samples of each readout integrated circuit (ROIC) type have been characterized in order to evaluate the device variability. The complete tested ROIC were designed and developed by Sofradir in the 0.25µm CMOS technology.

The first ROIC (called A) is designed for infrared detectors (IR), and the second ROIC (called B) is designed for near infrared detectors (NIR). Each ROIC controls three pixel arrays corresponding to three spectral bands. From design point of view, the main difference between the two ROICs is the size of the three bands. The total number of pixel for each ROIC is the same, but the number of columns and lines is different. For confidential reasons, the detailed pixel pitch and the characteristics of each spectral band will not be presented.

The different single events planned to be analysed during the irradiation campaign were based on the monitoring of two main signals of the ROIC: (a) the VIDEO signal (yellow line in Figure 2:) issued from the pixel selection table, (b) the DATAVALID signal of the ROIC.

Different signatures of SET were measured on the pixel tables during the test campaign. Two metrics were used to classify the SET events as illustrated in Figure 3: (a) the duration of SETs, (b) the multiplicity of SETs.

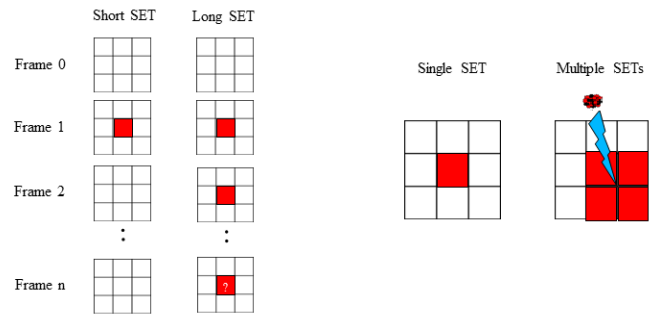


Figure 3: Classification of measured SETs: (a) as a function of its duration, (b) as a function of its multiplicity

Large and short SETs were defined as a function of the event duration observed on the VIDEO signal. If the SET event was observed during only one video frame, the SET event was called short SET. If the SET even was observed during two video frames of more, the SET event was called long SET.

Alongside, the multiplicity of SET was measured on the pixel table. The knowledge of SET multiplicity is very interesting to deduce the initial location of the event induced by the heavy ion on the ROIC (pixel table / row decoder ...). This point will be presented and discussed in the next sections.

### III. SINGLE EVENT EFFECTS RESULTS

#### A. Presentation of simple experimental SET data

Figure 4: and Figure 5: present the large SET cross sections measured on one sample of the readout devices “A” and “B”, respectively the samples A1 and B1. The total large SET cross section (black triangles), the large multiple SET (red squares) and the large single SET (blue diamonds) have been measured for a heavy ion with a LET of about  $32\text{MeV}\cdot\text{cm}^2/\text{mg}$  and for a range of temperatures from 50K up to 293K. The large multiple SETs cross sections are one decade lower than the large single SETs cross. Error bars were calculated and plotted for each cross section value. The statistical errors are very low because of the large events counts.

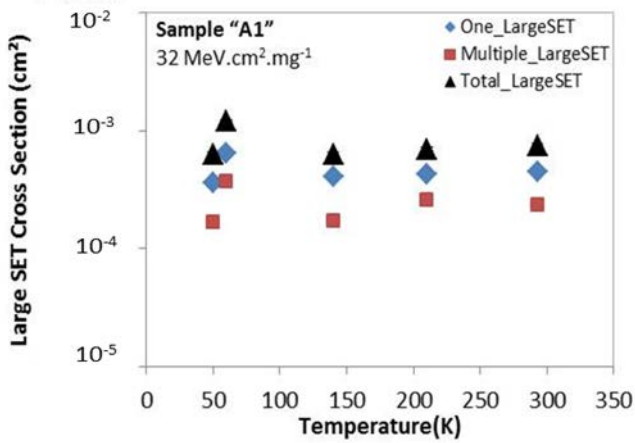


Figure 4: Large SET experimental cross sections measured on the sample “A1” during the test campaign under heavy ion ( $32\text{MeV}\cdot\text{cm}^2/\text{mg}$ ), as a function of temperature from 50K to 293K.

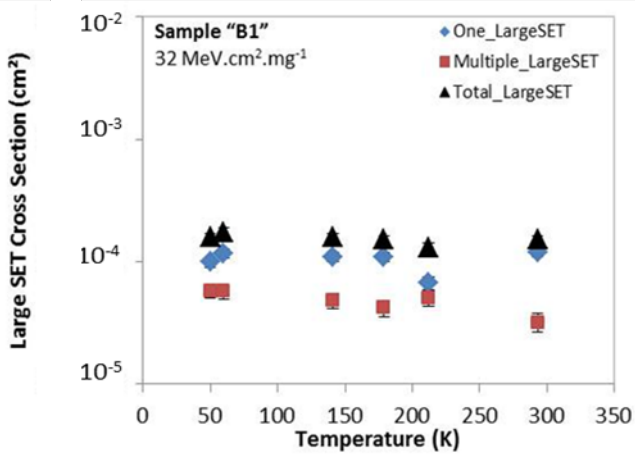


Figure 5: Large SET experimental cross sections measured on the sample “B1” during the test campaign under heavy ion ( $32\text{MeV}\cdot\text{cm}^2/\text{mg}$ ), as a function of temperature from 50K to 293K.

Fig. 3 and Fig. 4 present the short SET cross sections measured on one sample of the readout devices “A” and “B”, respectively the samples A1 and B1. The total short SET cross section (black triangles), the short multiple SETs (red squares) and the short single SETs (blue diamonds)

have been calculated for a heavy ion with a LET of about  $32\text{MeV}\cdot\text{cm}^2/\text{mg}$  and for a range of temperatures from 50K up to 293K. Note that short multiple SETs have been detected only for sample “A1” at 55K. This point is discussed in section III.B. Total SETs cross sections are very close to short single SETs cross sections. It means that, the occurrence probability of complex short SET events is very low. As previously, error bars were calculated and plotted for each value of cross section. The statistical errors are very low because of the large events counts.

The results highlight a limited temperature dependence of large and short SETs susceptibilities for the two ROICs. This trend is in good agreement with a previous work done on D-Flip Flop CMOS device, i.e., for temperatures down to 77 K [5]. This limited impact temperature has been highlighted in CMOS gates due to two reasons: (a) saturation of carrier mobility and (b) transistors threshold voltage [5].

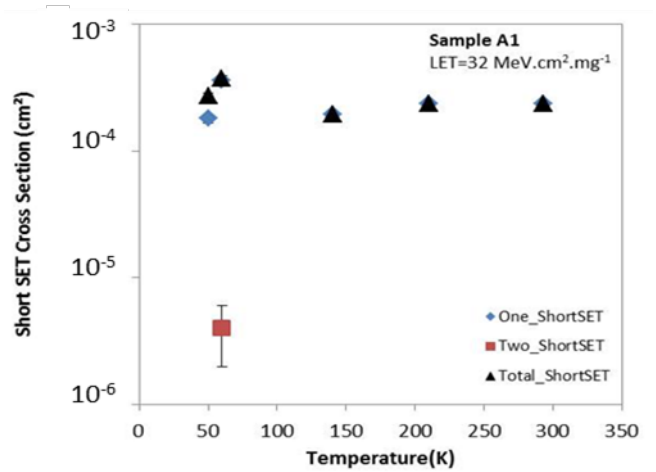


Figure 6: Short SET experimental cross sections measured on the sample “A1” during the test campaign under heavy ion ( $32\text{MeV}\cdot\text{cm}^2/\text{mg}$ ), as a function of temperature from 50K to 293K.

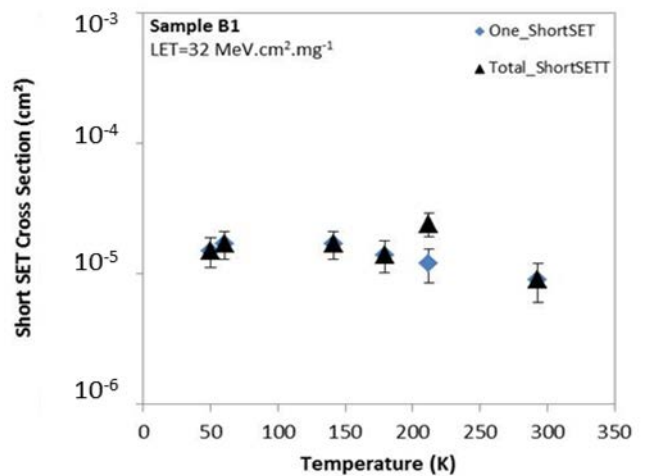


Figure 7: Short SET experimental cross sections measured on the sample “B1” during the test campaign under heavy ion ( $32\text{MeV}\cdot\text{cm}^2/\text{mg}$ ), as a function of temperature from 50K to 293K.

## B. Discussion of the multiplicity of simple SET

Figure 8: presents a histogram of large SET events depending on their multiplicity. Each bar of the histogram represents the number of large SET events on the sample "A1" during test campaign at 60K. It has been irradiated at a fluence  $1.10^6 \text{ cm}^{-2}$  with a heavy ion LET of about  $32 \text{ MeV} \cdot \text{cm}^2 / \text{mg}$ . As mentioned, the ROIC A contains three pixel arrays. The dimensions of the first array are  $224 \times 4$  pixels (line  $\times$  column). The second array is based on  $224 \times 4$  pixels. The third array is based on  $448 \times 4$  pixels. In this histogram, the single large SET events are the main events observed. The number of double large SET (120) is lower by a factor of three than the simple large SET numbers (369). The figure highlights the low probability to observe more than two events on the neighbourhood of a pixel. But the event with the seven multiple events during a single video frame seem to be not due to the strike of a heavy ion on the pixel arrays. In this histogram the category of events higher than 224 (the lower column size of pixel tables) is considered as complex SET events.

Finally, in order to confirm the hypothesis of the origin of the multiplicity of short and large SET an analysis has been performed by the mean of simulation based on the Monte Carlo SEE prediction tool, MUSCA SEP3 [3][4].

SEE prediction tools are used to analyse experimental data and confirm the hypotheses of the SEE experimental trends. Based on the design parameters of the pixel table provided by Sofradir, the SET sensitivity of the ROIC has been calculated by the mean of the tool MUSCA SEP3 [3][4]. The tool uses a Monte Carlo approach coupled in a sequential modeling all the physical and electrical processes, from the device down to the semiconductor target. The following steps are considered: (a) the modeling of the radiation constraint, (b) the transport mechanisms of radiation particles (in this work heavy ions) through the layer stack (BEOL) [7], (c) the generation of electron-hole pairs in the silicon, (d) the mechanisms of charges transport and collection, (e) the circuit feedback.

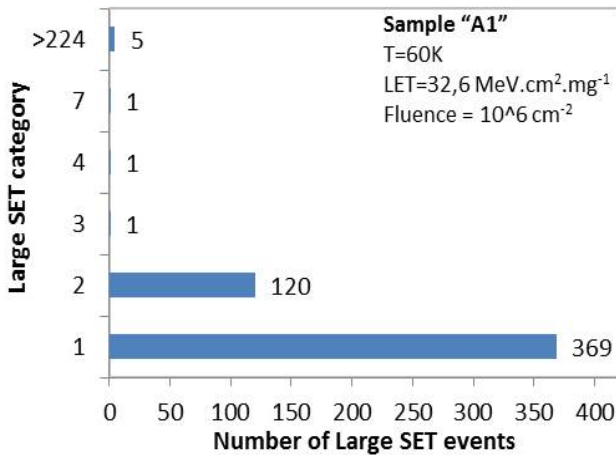


Figure 8: Number of Large SET events in each categories measured on the sample "A1" during the test campaign at 60K under heavy ion beam, fluence= $10^6 \text{ cm}^{-2}$ , LET= $32 \text{ MeV} \cdot \text{cm}^2 / \text{mg}$ .

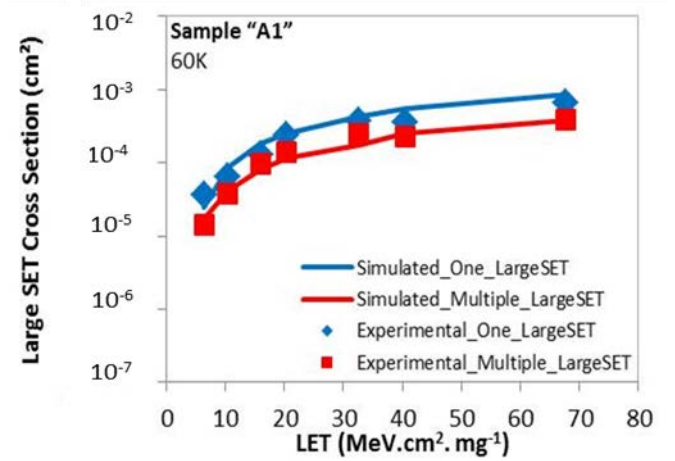


Figure 9: Comparison of large SET experimental cross section and simulations results from MUSCA SEP3 for the ROIC "A1", as a function of LET at 60K.

Figure 9: presents the SET cross sections calculated for sample "A1" under heavy ions. The multiplicity of the SET events is highlighted and it confirms that only two SET could be induced by a single particle in the pixel table for this technology. It means that the origin of events higher than four is due to events on the readout circuit, such as in a DFF of a line or column decoders of the pixel table.

Here, the analysis of short and large SETs of the pixel selection table (named simple SET) was presented. In the next section, the analysis of complex SET will be discussed.

## C. Presentation of complex experimental SET data

Here is presented complex large SET which has been defined as a SET event with a multiplicity higher than the length of a line and/or column of the pixel selection table. The comparison between simple (black squares) and complex (red dots) SET measured on the pixel array is presented in Figure 10:

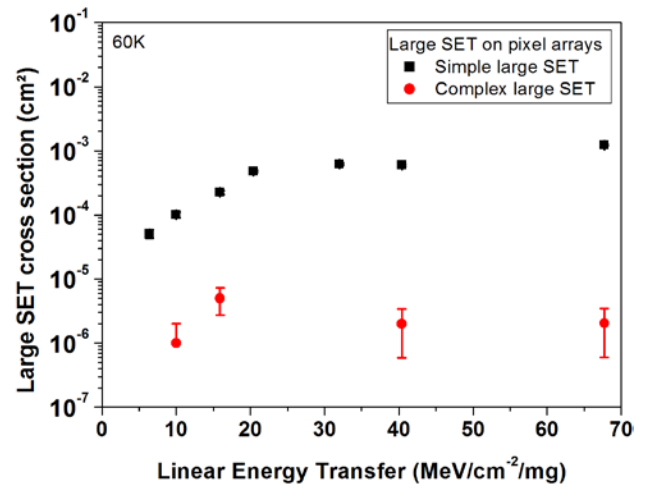


Figure 10: Comparison of simple (black squares) and complex (red dots) large SET obtained on pixel array of ROIC B as a function of LET during heavy ion irradiation at 60K

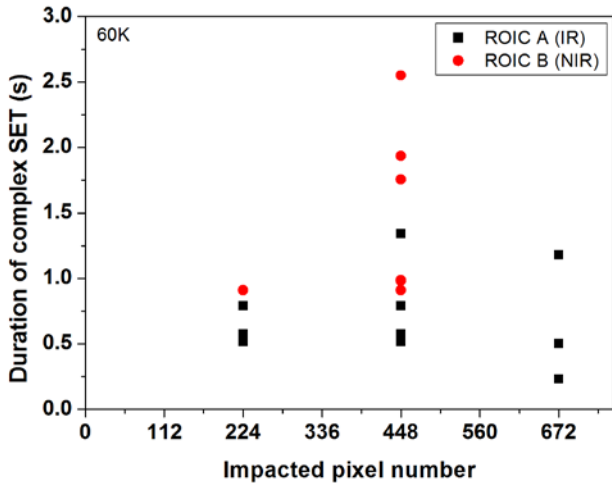


Figure 11: Duration of complex SET as a function the number of impacted pixel on ROIC A (black squares) and ROIC B (red dots) during heavy ion irradiation at 60K.

The occurrence of complex large SET is lower by a factor of about 2 orders of magnitude for all the investigated LET range. Even if the cross section of complex large SET is low, because of the critical impact of such complex SET, it is necessary to analyse these categories of event.

Figure 11: shows the characteristics (in terms of duration and impacted pixels) of complex large SETs observed on the ROIC A and ROIC B at 60K for heavy ions with a LET from 6.6 up to 67.7 MeV.cm<sup>2</sup>/mg. The event signatures must be identified as a function of the number of pixels affected by a complex long SET event. Three categories of error signature can be identified. The three event signatures correspond to multiples of number of lines of pixel arrays of the ROICs. The events have the same large SET signature which consists in a succession of 112, 224 or 448 large SETs during a single video frame. These complex large SETs correspond to a change of the level of all pixels of a column of the third pixel array of the ROIC B. These events can induce very long durations of video signal inoperability. Note that, the Video signal recovers its reference level without any on/off cycle.

This kind of complex large SET signature must be attributed to an event (such as SEU) on the vertical decoder of pixel arrays.

#### D. SEFI sensitivity of ROIC

In this section, two categories of SEFI are shown: SEFI on the VIDEO frame and SEFI on a multiplexer used in the control of the phase of the VIDEO signal.

Figure 12: shows the SEFI cross sections of the ROIC A obtained under heavy ions with LETs from 3.3 MeV/cm<sup>2</sup>/mg up to 67.7 MeV.cm<sup>2</sup>/mg at 60K. Note that same trend have been observed by ROIC B. The error bars correspond to statistic error of the measurements. A SEFI event corresponds to a change of state of the VIDEO signal during a frame. The SEFI sensitivity of the two ROIC designs seems to be quite

equivalent. It is interesting to note that the changes of state of the VIDEO signal request a power cycle (on/off) of the device in order to recover the reference pixel level. This kind of event should be due to an event on the configuration register used in the ROIC circuit. The other point which needs to be highlighted is the constant SEFI sensitivity as a function of the LET (Liner Energy Transfer). The LET threshold is about 6.6 MeV.cm<sup>2</sup>/mg. Note that the statistic is really poor.

Figure 13: shows the SEFI cross section obtained under heavy ions with LETs from 3.3 MeV/cm<sup>2</sup>/mg up to 67.7 MeV.cm<sup>2</sup>/mg for the design of ROIC A (black squares) and ROIC B (red dots). As previously, the error bars correspond to statistic error of the measurements. The SEFI event corresponds to a failure of the multiplexer or its configuration register. A wide variability of this SEFI type has been observed on the samples of the two ROIC; higher than one decade in some case. It seems that the design of the multiplexer and its configuration register is more sensitive to SEFIs for the ROIC B (NIR detector) than the ROIC A (IR detector). This difference is highlighted by the LET threshold which is increased by a factor of 2. The LET threshold of the ROIC A reaches 10 MeV.cm<sup>2</sup>/mg.

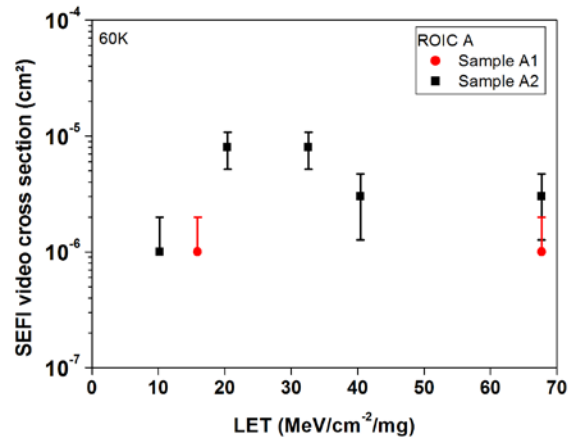


Figure 12: SEFI video cross section of two samples, A1 (red dots) and A2 (black squares) of the ROIC A design during heavy ion irradiation at 60K

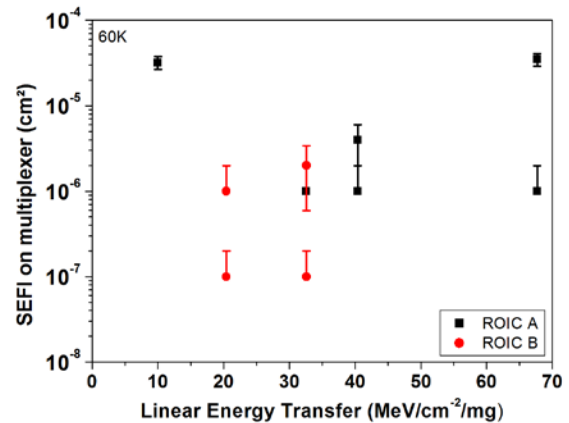


Figure 13: SEFI cross section of multiplexer of ROIC A (black squares) and ROIC B (red dots) under heavy ion irradiation at 60K

Figure 14: shows the effect of the temperature on the SEFI

video cross section obtained for two samples of the ROIC A design, the sample A1 (black squares) and the sample A2 (red dots) for a heavy ion beam with a LET of about  $67.7 \text{ MeV}\cdot\text{cm}^2/\text{mg}$ . As previously, the error bars correspond to statistic error of the measurements. No temperature dependence can be observed. This point is also confirmed for other LETs and design B of the ROIC.

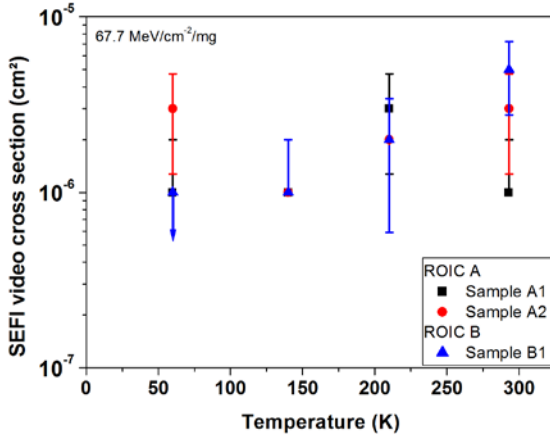


Figure 14: Effect of temperature of the SEFI cross section of ROIC A (black squares, red dots) and ROIC B (blue triangles) under heavy ion irradiation at 60K

Experimental data confirmed the very limited impact of the cryogenic temperature on SEE occurrence on the two ROICs [7][8]. These results are consistent with previous simulation results on elementary gates (DFF) [5][6].

#### IV. CONCLUSION

This work presented the analyses of single event transients and functional interrupts measured on two designs of readout integrated circuit under a heavy ions beam cooled down at cryogenic temperatures. The analysis of the multiplicity of SETs in the pixel arrays was completed by means of the SEE prediction tool, MUSCA SEP3. Experimental data confirmed the very limited impact of the cryogenic temperature on SEE occurrence on the two ROICs. These results are consistent with previous simulation results on elementary gates (DFF). It appears that for this technology used by Sofradir for their ROIC of IR detectors, the future irradiation test campaigns should be realized at room temperature. This allows for reducing the complexity of such irradiation tests during the development of IR detector for a space mission.

#### V. REFERENCES

- [1] G. R. Hopkinson, 2000, Dec. Proton-induced changes in CTE for n-channel CDDs and the effect on star tracker performance, IEEE Transaction on Nuclear Sciences.
- [2] C. Virmontois et al, 2014, Dec. Radiation-induced dose and single event effects in digital CMOS image sensors, IEEE Transaction on Nuclear Sciences.
- [3] G. Hubert, et al, 2009, Dec. Operational SER calculations on the SAC-C orbit using the multi-scales single event phenomena predictive plat-form (MUSCA SEP3 IEEE Transaction on Nuclear Sciences.
- [4] G. Hubert, et al, 2013, Dec. Single-event transient modeling in a 65-nm bulk CMOS technology based on multi-physical approach and electrical simulations, IEEE Transaction on Nuclear Sciences.
- [5] L. Artola et al, 2015, Dec. Single Event Upset Sensitivity of D-Flip Flop of Infrared Image Sensors for Low Temperature Applications Down to 77 K, IEEE Transaction on Nuclear Sciences.
- [6] L. Artola et al, 2018, Impact of D-Flip-Flop Architectures and Designs on Single Event Upset Induced by Heavy Ions, IEEE Transaction on Nuclear Sciences.
- [7] L. Artola et al, 2017, Single Event Transient and Functional Interrupt in Readout Integrated Circuit of Infrared Image Sensors at Low Temperatures, IEEE Radiation Effects Data Workshop (REDW)
- [8] A. Al Youssef, et al, 2018 Jan., Single-Event Transients in Readout Circuitries at Low Temperature Down to 50 K, IEEE Transaction on Nuclear Sciences.